ELSEVIER

Biochimica et Biophysica Acta 1329 (1997) 357–369

BIOCHIMICA ET BIOPHYSICA ACTA
BBA

Effects on mollicutes (wall-less bacteria) of synthetic peptides comprising a signal peptide or a membrane fusion peptide, and a nuclear localization sequence (NLS) – a comparison with melittin

Laure Béven [a], Laurent Chaloin [b], Pierre Vidal [b], Frédéric Heitz [b], Henri Wróblewski [a,*]

[a] *Groupe 'Membranes et Osmorégulation', UPRES-A CNRS No. 6026, GDR CNRS No. 1153, Université de Rennes 1, Campus de Beaulieu, Bâtiment 14, 35042 Rennes Cedex, France*

[b] *CRBM-CNRS ERS No. 155, GDR CNRS No.1153, BP 5051, 34033 Montpellier, France*

Received 7 April 1997; revised 21 May 1997; accepted 26 May 1997

Abstract

In order to investigate the effect of primary amphipathic peptides on mollicutes (wall-less bacteria), we have synthesised five molecules (P1, P2, P3, JM123, and JM133) comprising a 16 to 18-residue hydrophobic sequence and the nuclear localization sequence (NLS) PKKKRKV of simian virus 40 large-T antigen, *C*-terminated by a cysteamide group. The hydrophobic cluster was in P1 the signal sequence of the heavy chain of *Caiman crocodilus* immunoglobulin G and in JM123 the fusion peptide of human immunodeficiency virus 1 glycoprotein gp41 in which phenylalanine[7] was replaced by a tryptophan residue. The homologues P2, P3, and JM133 were obtained by slight alterations of these sequences. Circular dichroism spectroscopy revealed that, in liposomes, P-series peptides were mainly under the form of β-sheets whereas JM-series peptides displayed a high proportion of turns. These peptides proved to be bactericidal for some mollicutes, notably *Acholeplasma laidlawii*, but were much less potent than melittin. Furthermore, their antibiotic activity was independent of the average thickness of the plasma membrane hydrophobic core whilst that of melittin was inversely related to the thickness. Melittin and the synthetic peptides abolished spiroplasma cell motility and helicity, but only melittin and P-series peptides split the cells into globular forms displaying an average diameter of ca. 1 μm. In contrast to melittin, the synthetic peptides agglutinated spiroplasmas, suggesting that their polycationic NLS was exposed on the cell surface. P-series peptides decreased, though less efficiently than melittin, *A. laidlawii* and *Spiroplasma melliferum* membrane potential ($\Delta\Psi$) and transmembrane pH gradient (ΔpH), at concentrations much lower than their minimal inhibitory concentrations whilst JM-series peptides had no effect on $\Delta\Psi$ and ΔpH in the same conditions. Actually, the bactericidal

Abbreviations: A_{600}, light absorbance at 600 nm; CD, circular dichroism; CFU, colony forming unit; cFDASE, 5(6-)-carboxyfluorescein diacetate succinimidyl ester; cFSE, 5(6-)-carboxyfluorescein succinimidyl ester; $diSC_3$-(5), 3,3′-dipropyl-2,2′-thiadicarbocyanine iodide; DOPG, dioleylphosphatidyl glycerol; Fmoc, fluorophenyl methoxycarbonyl; Hepes, (hydroxy-2-ethyl-4-piperazinyl-1)-2-ethane sulfonic acid; MIC, minimal inhibitory concentration; NEM, *N*-ethyl morpholine; NLS, nuclear localization sequence; SUV, small unilamellar vesicles; Tris, Tris-(hydroxymethyl)-aminomethane; ΔI, change in fluorescence intensity; ΔpH, transmembrane pH gradient ($\Delta pH = pH_{in} - pH_{out}$); $\Delta\Psi$, membrane electrical potential ($\Delta\Psi = \Psi_{in} - \Psi_{out}$)

* Corresponding author. Fax: +33-299286700.

PII S0005-2736(97)00130-2

activity of these peptides towards mollicutes was proportional to their ability to collapse the electrochemical transmembrane potential. © 1997 Elsevier Science B.V.

Keywords: Acholeplasma; Amphipathic peptide; Cell deformation; Growth inhibition; Membrane potential; Membrane thickness; Melittin; Mollicute; Mycoplasma; Spiroplasma

1. Introduction

The most widely used defence system in nature is that involving peptides since it seems to be shared by all living organisms, from the simplest (bacteria) to the most complex (plants and animals) (for recent reviews see [1–8]). Though these peptide weapons display very diverse sequences, they are most often short (less than 40 residues), cationic, and amphiphilic. They may be classified within two distinct groups: ribosomally synthesised peptides and peptides synthesised by multienzymatic (nonribosomal) systems. Ribosomally synthesised peptides of eucaryotes are linear, composed of only standard L-amino acids, and contain disulfide bonds (e.g., defensins) or not (e.g., cecropins). Those synthesised by bacteria (lantibiotics) contain lanthionine thioether bonds. Nonribosomally synthesised peptides (for review see [9]) may be linear (e.g., peptaibols) or cyclic (gramicidin S). The former contain unusual residues (e.g. α-aminoisobutyric acid) and the latter D-amino acids; both may be acylated. Most of these attack/defence molecules are membranotropic: Their main target is indeed the cell plasma membrane in which they insert and alter permeability. Many of them have thus been described as ionophores forming transmembrane ion channels (e.g., alamethicin) or acting as shuttle carriers (e.g., valinomycin). However, as in the case of melittin, peptide antibiotic activity may also be based upon more complex membrane structural disorders [10] (for a review see [11]).

Linear peptides composed of standard L-amino acids are particularly suited for experimental research since they are easier to chemically synthesise than peptides containing unusual residues. Furthermore, it is possible to conceive a large number of variants for investigating structure/activity relationships (enantio, retro, and retroenantio isomers, deletions, insertions, etc.). In this category, the amphipathic cationic α-helix is the archetype of the pore-forming antibiotic peptide [11,12]. Hence, it is not surprising that a large amount of research has been devoted to peptides of this specific category in contrast to primary amphipathic peptides, i.e., those in which the hydrophobic residues and the hydrophilic ones are segregated along the sequence within two distinct clusters. We have recently synthesised five linear peptides comprising a 16 to 18-residue hydrophobic sequence corresponding to a signal sequence or to a membrane fusion peptide, linked to the NLS (nuclear localization sequence) PKKKRKV [13,14], *C*-terminated by a cysteamide group (Fig. 1). Though these peptides were initially designed for the vectorisation of drugs in animal cells, they provided the opportunity of investigating the effects of primary amphipathic peptides on bacterial cells.

Mollicutes were chosen as target bacteria because they represent the simplest, cultivable, and self-replicating organisms described thus far [15–17]. Their cell envelope is composed of only the plasma membrane which should facilitate the analysis of the interactions between peptides and the bacterial cell surface. We have recently shown that mollicutes are much more sensitive to amphipathic peptides produced by bacteria (gramicidin S, valinomycin, globomycin, iturin, and surfactin) and fungi (alamethicin) than to animal defence peptides such as cecropins and magainin [18,19]. We believe that this is probably one of the main reasons why mollicutes successfully parasite such a wide range of eucaryotic hosts as plants, insects and mammals including humans.

In this work, we have analysed the conformation of these synthetic peptides in different conditions, using circular dichroism spectroscopy (CD). Their antibacterial activity was assessed by the growth

P1	*Ac* M G L G L H L L V L A A A L Q G A W S Q P K K K R K V Cya
P2	*Ac* M G L G L H L L - L A A A L Q G A - - - - K K K R K V Cya
P3	*Ac* M G L G L H L L V L A A A L Q G A - - - - K K K R K V Cya
JM123	*Ac* G A L F L G W L G A A G S T M G A R - - - K K K R K V Cya
JM133	*Ac* G A L F L G W L G A A G S T M G A W S Q P K K K R K V Cya
Mellitin	G I G A V L K V L T T G L P A L I S W I K R K R Q Q *NH2*

Fig. 1. Sequences of melittin and of the five synthetic peptides studied in this work.

inhibition method whereas the effects on cell shape and motility, and on the transmembrane electrochemical potential were analysed using dark-field light microscopy and spectrofluorometry. Bee-venom melittin [20], a secondary amphipathic peptide displaying a strong bactericidal activity, was used for comparison.

2. Materials and methods

2.1. Commercial lipids and peptides

Dioleylphosphatidylglycerol (DOPG), valinomycin, nigericin, and ultrapure melittin were purchased from Sigma (St. Louis, MI).

2.2. Peptide synthesis

The synthesis of the peptides was performed on aminoethyldithio-2-isobutyric acid-Expansin with a Milligen 9050 Pepsynthetizer (Millipore, UK) with the Fmoc (fluorophenyl methoxycarbonyl)/tertiobutyl system as described previously [21,22] and according to manufacturer's instructions. Fmoc amino acids were activated by the addition of equimolar amounts of *O*-(1*H*-benzotriazol-1-yl)-*N*,*N*,*N*,*N*-tetramethyl-uroniumtetrafluoroborate and 1-hydroxybenzotriazole diluted to 0.3 M with 5.5% *N*-ethyl morpholine in *N*,*N*-dimethylformamide. Coupling was obtained by running this solution through the reaction column for 45 min. Double couplings (45 min) were performed at crucial steps (Thr^{14}, Ala^{17}, Arg^{18}, Lys^{21}, Arg^{22}, and Val^{24}) to improve yield and make purification easier. Fmoc deprotection was achieved by percolating 20% piperidine in *N*,*N*-dimethylformamide through the reaction column for 4.5 min at 3.8 ml min^{-1} for the first nine cycles and 1 min at 3.8 ml min^{-1} plus 7 min at 1.5 ml min^{-1} for the end of the synthesis. After deprotection of the terminal amino group, the side chain-protected peptidyl resin was washed four times with dichloromethane and four times with diethylether, and finally was dried under vacuum [23].

2.3. Peptide purification and analysis

The peptides were purified by analytical HPLC on an Aquapore (Applied Biosystems, San Jose, CA) RP 300 column (C8, 7 μm, 4.6 × 220 mm) and by semi-preparative HPLC on a Nucleosil (SFCC, Neuilly-Plaisance, France) 300 column (C18, 5 μm, 20 × 200 mm). Electrospray mass spectrometric analyses were carried out in the positive ion mode using a Trio 2000 VG Biotech Mass Spectrometer (Altringham, UK). Amino acid analyses were performed on a Model 7300 high performance analyser (Beckman Instruments, Fullerton, CA) and Gold software was used for the quantification. Typically, 50 nmol of peptide was hydrolysed under vacuum in sealed glass tubes in 0.2 ml of 5.7 N HCl containing 0.9% phenol, at 110°C for 23 and 46 h. For tryptophan determination, hydrolysis was performed in 4 M methane sulfonic acid for 24 h.

2.4. Circular dichroism spectroscopy

Circular dichroism (CD) measurements of peptide solutions were recorded from 190 to 260 nm at 20°C with a Jobin–Yvon Mark V dichrograph at a scan speed of 20 nm min^{-1} in 0.1 mm (peptides in SDS) or 1 mm (peptides in water or liposomes) path length quartz cells. The peptides were analysed in 10 mM sodium phosphate buffer (pH 7.2) containing or not SDS or liposomes (see Fig. 2 for details). 5 scans were performed per analysis and subsequently averaged. Corrections were made for buffer and detergent or lipid contribution. The Dicroprot software v2.3d (Gilbert Deleage, IBCP Lyon, France) was used for evaluating percentages of α-helix, β-sheet, turn and random coil contents. The fit results were obtained by a least square method based on the Gauss–Jordan elimination.

2.5. Preparation of vesicles

Small unilamellar vesicles (SUV) were prepared from DOPG by sonication. Briefly, dry lipids were dissolved in chloroform/methanol (3:1, vol/vol). The solvent was evaporated under a nitrogen stream and the sample desiccated under high vacuum for at least 3 h to remove residual solvent. The lipids were resuspended in buffer (2 mg ml^{-1}) by vortex mixing and sonicated (ca. 20 min at 80% pulse cycle in an ice/water bath) with a probe sonicator. All SUV preparations were equilibrated overnight at 4°C before use.

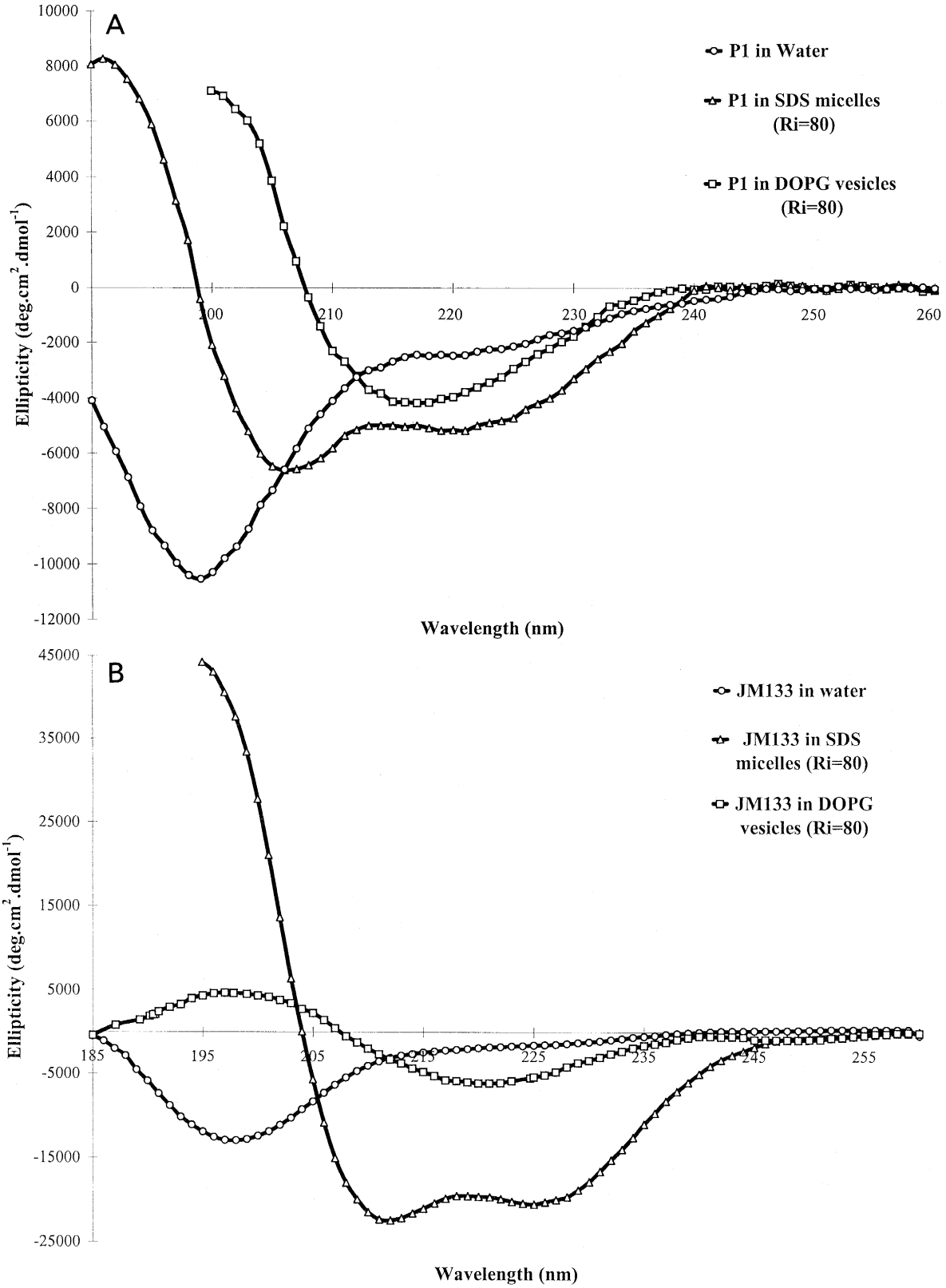
A
P1 in Water
P1 in SDS micelles (Ri=80)
P1 in DOPG vesicles (Ri=80)
Ellipticity (deg.cm^2.dmol^{-1})
Wavelength (nm)
B
JM133 in water
JM133 in SDS micelles (Ri=80)
JM133 in DOPG vesicles (Ri=80)
Ellipticity (deg.cm^2.dmol^{-1})
Wavelength (nm)

2.6. Bacterial strains and growth conditions

The seven strains of mollicutes used in this study were *Acholeplasma laidlawii* A-PG8, *A. laidlawii* A-EF22, *M. gallisepticum* S6, *M. genitalium* G37, *M. mycoides* ssp. *mycoides* SC KH3J, *S. citri* R8A2, and *S. melliferum* BC3. In most experiments, these bacteria were cultured as described previously [19]. Furthermore, in order to determine the influence of the average thickness of the hydrophobic core of the cell membrane on peptide antibiotic activity, *A. laidlawii* A-EF22 was adapted to and grown in lipid-free media with defined fatty acid content, as described previously [24] (see Table 3 for details).

2.7. Determination of minimal inhibitory concentrations (MICs)

The mollicutes were cultured under microaerobic conditions in appropriate liquid media as described previously [18,19]. Minimal inhibitory concentrations (MICs) were determined by culturing the cells in 96-well microtitration plates in the presence of 2-fold serial dilutions of the peptides and following the colour change of phenol red resulting from the acidification of the culture medium during the growth. The starting cell concentration was 10^6 colony-forming units (CFU) ml^{-1} and the assays were performed in triplicate. Organisms were considered resistant when their growth could not be prevented by peptide concentrations up to 100 μM. To distinguish bacteriostatic effects from bactericidal ones, cells were incubated in the presence of peptides for 2 h and plated on solid culture medium containing 1% noble agar. The plates were subsequently incubated and examined daily for the apparition of colonies.

2.8. Light microscopy

Exponentially growing *S. melliferum* BC3 cells were sedimented by centrifugation at $10\,000 \times g$ for 10 min at 4°C and dispersed in 50 mM sodium phosphate buffer (pH 7.0) containing 50 mM D-glucose and 549 mM D-sorbitol. The suspension contained 10^{10} CFU ml^{-1} (absorbance, $A_{600} = 1.0$). The effect of peptides on spiroplasma cell morphology and motility was observed with a Leitz Diaplan microscope equipped with a 100-W halogen lamp, Leitz oil immersion dark-field condenser (NA 1.2 to 1.4), Leitz PL Fluotar 100× objective (NA 0.6 to 1.32), and Periplan GF 12.5×/18M eyepieces. A volume of 10 μl of cell suspension was deposited on a glass slide ($1 \times 25 \times 75$ mm) and covered with a glass coverslip of $0.15 \times 24 \times 36$ mm. Micrographs were taken with a Nikon F-801 camera using Kodak T-Max 35 mm film (ISO 3200). Spiroplasma cells treated or not with peptides were also fixed with 2.5% glutaraldehyde (pH 7.0), spread on glass slides, stained with crystal violet, and observed as described for live cells. In this latter case, micrographs were taken using Ilford HP 5 Plus 35 mm film (ISO 400).

2.9. Fluorescence measurements of the effect of peptides on cell membrane potential

Fluorescence studies were performed as described previously [18,19,25] on *A. laidlawii* A-PG8 and *S. melliferum* BC3. Alterations of membrane potential by peptides were probed using the fluorescent carbocyanine dye $diSC_3$-(5) (3,3′-dipropyl-2,2′-thiadicarbocyanine iodide) [26]. Exponentially growing *A. laidlawii* cells were harvested, washed once and dispersed in 5 mM (hydroxy-2-ethyl-4-piperazinyl-1)-2-ethane sulfonic acid pH 7.0 (Hepes buffer, 150 mM NaCl) to obtain a cell density of 10^9 CFU ml^{-1} ($A_{600} = 0.06$; 20 μg of cell protein ml^{-1}). Similarly, *S. melliferum* cells were washed and dispersed in 5 mM Hepes buffer (pH 7.0, 128 mM NaCl) to obtain a cell density of 10^9 CFU ml^{-1} ($A_{600} = 0.10$, 30 μg of cell protein ml^{-1}). In these conditions, *S. melliferum* cells conserved their helical morphology and motility for about 30 min. A freshly prepared 0.15 mM methanol solution of $diSC_3$-(5) was added to the cell suspensions (3 ml) at a final concentration of 0.15

Fig. 2. Circular dichroism spectra of peptides P1 (A) and JM133 (B) in different media. Peptides were solubilised in buffer (○), buffer containing 40 mM SDS (△), or in buffer containing 3.1 mM DOPG (□). All the measurements were performed in 10 mM sodium phosphate buffer (pH 7.2). The concentration of SDS was well above its critical micelle concentration (CMC = 8 mM in the same experimental conditions). R_i, detergent or lipid/peptide molar ratio.

μM. The fluorescence signal was measured with a Kontron SFM 25 spectrofluorometer equipped with a magnetic stirring holder using 5 ml quartz cuvettes (1 cm path length) maintained at 37°C for *A. laidlawii* and 32°C for *S. melliferum*. Excitation and emission wavelengths were set at 625 and 660 nm, respectively. When steady-state fluorescence levels were obtained, 3 μl of peptide solution in water (melittin), methanol (melittin, valinomycin, P1, P2, P3), or dimethylsulfoxide/methanol 1:9 (vol/vol) (JM 123, JM133) was added to the cell suspension. The peptides were used at final concentrations ranging from 0 to 0.1 μM. The solvents for peptide and dye solubilisation did not interfere at the concentrations used (i.e., $\leq 0.2\%$, vol/vol).

The calibration of dye fluorescence change ($\%\Delta I$) vs. change of membrane electrical potential ($\Delta\Psi$) was performed using valinomycin-induced K^+ diffusion potential [27]. This potential was calculated from the Nernst equation $\Delta\Psi = (RT/F)\log([K^+]_{in}/[K^+]_{out})$ where $[K^+]_{in}$ and $[K^+]_{out}$ are the known initial potassium ion concentrations. Potassium was determined by flame spectrometry. Intracellular volume was determined by the method of Stock et al. [28] using [*carboxyl*-^{14}C]inulin (111 MBq g^{-1}) (DuPont NEN, Boston, MA) and ^3H_2O (400 MBq ml^{-1}) (Amersham, Les Ulis, France) as markers. Spiroplasma cells were centrifuged at $10\,000 \times g$ for 10 min and the pellets were dispersed in 5 mM Hepes buffer (440 mM D-sorbitol and 128 mM NaCl) to obtain an A_{600} of 5. Samples (500 μl) of this suspension were incubated for 30 min in the presence of radiolabelled inulin (10^5 dpm) or with tritiated water (10^6 dpm) to determine extracellular and total volumes of the pellets, respectively. Radioactivity was determined by liquid scintillation counting.

2.10. Determination of intracellular pH

The intracellular pH of mollicutes (pH_{in}) was determined with the internally conjugated fluorescent probe 5(6-)-carboxyfluorescein succinimidyl ester (cFSE, [29]). Bacteria were grown, harvested, and dispersed to obtain 10^{10} CFU ml^{-1} of 50 mM potassium-phosphate buffer pH 7.4 containing 150 mM NaCl (*A. laidlawii*) or 549 mM D-sorbitol (*S. melliferum*). The cells were then incubated in the presence of 1.0 μM 5(6-)-carboxyfluorescein (cFDASE). After 10 min, the cells were washed and incubated for further 30 min in the presence of 10 mM glucose to remove nonconjugated cFDASE. Cells containing the fluorescent probe were diluted 10× and 3 ml were transferred in a 5-ml quartz cuvette placed in a stirred and thermostated holder in the spectrofluorometer. Fluorescence intensities were recorded at an emission wavelength of 520 nm whereas the excitation was set at 490 nm. The 490-to-440 nm ratios were corrected for background signal due to buffer. The incubation and recording temperatures were 32°C for *S. melliferum* and 37°C for *A. laidlawii*. At the end of each assay, the extracellular fluorescence signal was determined in cell filtrates (pore diameter, 0.1 μm). Calibration curves for pH_{in} were determined in buffers with pH_{out} values ranging from 5 to 8. Buffers were prepared from glycine (50 mM), citric acid (50 mM), Na_2HPO_4–$2H_2O$ (50 mM), and KCl (50 mM) with pH being adjusted with HCl or NaOH. In the case of *S. melliferum*, the buffered solutions contained 440 mM D-sorbitol as osmoprotectant. The pH_{in} and pH_{out} were equilibrated by addition of 2 μM valinomycin and 2 μM nigericin, and the ratios were determined as described before.

2.11. Protein determination

Protein was determined with the method of Lowry et al. [30] modified by Markwell et al. [31], using bovine serum albumin as standard.

3. Results

3.1. Sequences and conformations of the peptides

The sequences of the five synthetic peptides are given in Fig. 1. P1 consisted in the hydrophobic signal sequence of the heavy chain of *Caiman crocodilus* immunoglobulin G and the NLS PKKKRKV of simian virus 40 large-T antigen [13,14], separated by a SQ dipeptide linker. The NLS was *C*-terminated by a cysteamide group. JM133 differed from P1 by the hydrophobic sequence (first 18 residues) which was the fusion peptide of human immunodeficiency virus 1 glycoprotein gp41 [32] in

which phenylalanine[7] and arginine[18] were replaced by tryptophan residues (W). As compared with JM133, JM123 conserved arginine[18] but missed the tripeptide SQP. In comparison with P1, P3 missed the sequence WSQP whereas P2 further missed valine[9]. These peptides were analysed by CD spectroscopy to determine their secondary structure in different media. The data listed in Table 1 were deduced from the CD spectra of P1 (Fig. 2A) and JM133 (Fig. 2B). In water, P1 appeared to be mainly disordered (69% coil) whereas in the presence of SDS micelles the proportion of ordered structures was increased (44% α-helix and 13% β-sheet) to the expense of coil (43%). However, in the presence of DOPG liposomes (SUV), the proportion of β-sheet was considerably increased since it reached 80%. No turn could be detected within P1 in any of the three media. In comparison, JM133 was essentially under the form of coil (60%) and β-sheet (40%) in water whereas in SDS micelles and in DOPG liposomes turns appeared to be the dominant conformation (50 and 63%, respectively). The spectra of P2 and P3 obtained in the same conditions were quite similar to those of P1 and the spectra of JM133 were identical to those obtained with JM123 (not shown).

3.2. Effect of the peptides on the growth of mollicutes

Melittin inhibited the growth of the six strains of mollicutes, with MICs ranging from 0.78 to 12.5 μM whereas the synthetic peptides proved much less potent (Table 2). JM123 and JM133 inhibited only *A. laidlawii* and *M. genitalium* with MICs ranging from 12.5 to 50 μM. P-series peptides proved capable of inhibiting all the mollicutes, except *M. mycoides* ssp. *mycoides* SC, with MICs ranging from 6.25 to 100 μM. Plating peptide-treated cells on solid medium revealed that in all cases where inhibition occurred, the synthetic peptides, similar to melittin, were bactericidal in spite of their lower activities.

Since *A. laidlawii* can be restricted to incorporating fatty acids from the growth medium into its

Table 1
Secondary structure (relative %) of peptides P1 and JM133 in different media as determined by CD spectroscopy

Peptide	Helix	β-Sheet	Turn	Coil
P1 in water	3	28	0	69
P1 in SDS	44	13	0	43
P1 in DOPG liposomes	9	80	0	11
JM133 in water	0	40	0	60
JM133 in SDS	24	13	50	13
JM133 in DOPG liposomes	9	5	63	23

Measurements were performed in 10 mM sodium phosphate buffer (pH 7.2) containing or not SDS or DOPG. See Fig. 2 for experimental conditions.

Table 2
Antibiotic activity of peptides JM123, JM133, P1, P2, and P3 on mollicutes, as compared with melittin

Peptides	*Al*	*Mgl*	*Mgn*	*Mm*	*Sc*	*Sm*
Melittin	0.78	6.25	6.25	12.5	0.78	1.56
JM123	25	R	50	R	R	R
JM133	12.5	R	50	R	R	R
P1	25	100	50	R	100	100
P2	6.25	50	50	R	100	100
P3	6.25	50	50	R	100	100

Data are expressed as minimal inhibitory concentrations (MICs) in μmol l^{-1}. Mollicutes were considered resistant (R) when they were not inhibited by concentrations up to 100 μM. Abbreviations: *Al*, *A. laidlawii*; *Mgl*, *M. gallisepticum*; *Mgn*, *M. genitalium*; *Mm*, *M. mycoides* ssp. *mycoides* SC; *Sc*, *S. citri*; *Sm*, *S. melliferum*. The same MICs were obtained for both strains (A-PG8 and A-EF22) of *A. laidlawii*.

Table 3
Influence of *A. laidlawii* A-EF22 membrane thickness on the antibiotic activity of melittin, JM123, JM133, P1, P2, and P3

Peptides	Average thickness of the hydrophobic core of the membrane (Å)			
	23 [a]	25 [b]	26.3 [c]	28 [d]
Melittin	0.78	0.78	1.56	3.12
JM123	25	25	25	25
JM133	12.5	12.5	12.5	12.5
P1	25	25	25	25
P2	6.25	6.25	6.25	6.25
P3	6.25	6.25	6.25	6.25

Data are expressed as μM minimal inhibitory concentrations (MICs). In order to obtain the indicated thicknesses, *A. laidlawii* A-EF22 was grown in lipid-free medium supplemented with:
[a] 75 μM tetradecanoic acid (14:0) + 75 μM *cis*-9-tetradecanoic acid (14:1c).
[b] 150 μM *cis*-9-hexadecanoic acid (16:1c).
[c] 150 μM *cis*-9-octadecanoic acid (18:1c).
[d] 150 μM *cis*-9-octadecanoic acid (18:1c) + 20 μM cholesterol.
These conditions give the following compositions in membrane lipids: (a) 14:0 + 14:1, molar ratio, 1/1, (b) 100% 16:1c, (c) 100% 18:1c, and (d) 18:1c + cholesterol, molar ratio 75/25 [24].

membrane lipids, this mollicute was grown under conditions that allowed membranes with four different hydrophobic core thickness to be obtained: 23, 25, 26.3, and 28 Å (Table 3). These figures were previously determined by ^{2}H-NMR spectroscopy [24]. In contrast to melittin which inhibitory activity decreased with increasing the thickness of the bilayer hydrophobic core from 23 to 28 Å, the activities of the five peptides were independent of membrane thickness. It should be stressed, however, that even in the case of the thickest cell membrane, the bactericidal activity of melittin was still very high (MIC = 3.12 μM).

3.3. Effect of the peptides on spiroplasma motility and cell morphology

Exponentially growing *S. melliferum* BC3 cells exhibited an average helix length of 6.5 ± 1.6 μm with a pitch of about 1 turn μm^{-1}. Upon treatment with melittin, the cells progressively lost their motility and helical shape. After 5 min of incubation in 0.1 μM melittin, the whole population (10^{10} CFU ml^{-1}) was transformed into spherical forms having an average diameter of about 1 μm (Figs. 3 and 4). The same phenomenon occurred within only a few seconds when the cells were treated with 1 μM melittin. P-series peptides exhibited the same deforming activity but the rates of deformed cells were of 70% and 90% after treatment with 10 and 100 μM peptide, respectively. The activity of JM123 was identical to that of JM133 but lower than the activities of the P-series peptides: About 60% of the cells were deformed after 10 min of treatment with 100 μM concentrations (Fig. 4). Furthermore, JM-series peptides proved unable to split the cells into spherical forms.

When the spiroplasma concentration was raised up to 10^{11} CFU ml^{-1}, treatment with either of the synthetic peptides induced a massive agglutination of deformed but still filamentous cells (Fig. 3), a phenomenon which was never observed with melittin. The average size of the cells indicated than no spiroplasma cell fusion occurred upon peptide treatment, even when using JM-series peptides which contain a hydrophobic membrane fusion sequence.

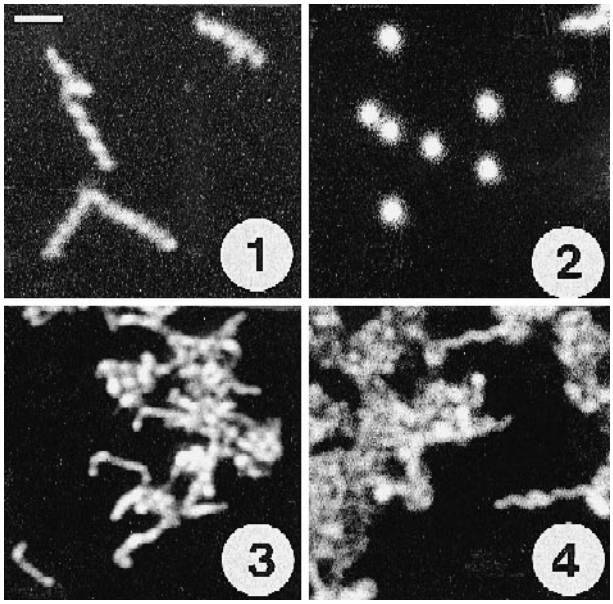

Fig. 3. Dark-field light microscopy observation of spiroplasma cell deformation. Untreated *S. melliferum* BC3 cells (1) are compared with cells treated with 0.1 μM melittin (2), 10 μM P1 (3), 10 μM JM133 (4). Cell densities were 10^{10} CFU ml^{-1} (1 and 2) and 10^{11} CFU ml^{-1} (3 and 4). See text for details. Bar (top left corner in 1), 2 μm.

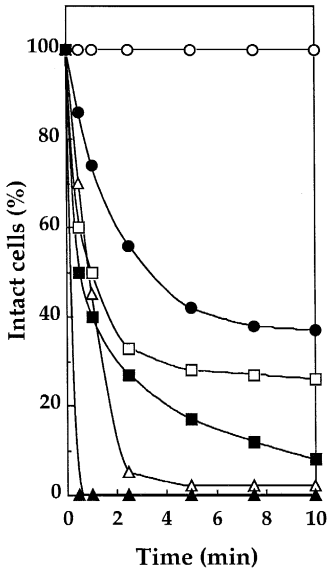

Fig. 4. Time-course of spiroplasma cell deformation by melittin, P1, and JM133. Cells were considered deformed when helicity was lost. Whenever cell deformation occurred, it was always preceded by the lost of cell motility. Each curve is the average of at least three independent measurements (standard deviation, SD ≤ ±5%). Symbols: untreated cells (○) and cells treated with 100 μM JM 133 (●), 10 μM P1 (□), 100 μM P1 (■), 0.1 μM melittin (△), or 1 μM melittin (▲).

3.4. Effect of the peptides on membrane potential

In order to quantitatively determine the transmembrane electrical potential ($\Delta\Psi$) in *A. laidlawii* A-PG8 and *S. melliferum* BC3, we have first correlated the relative fluorescence quenching (ΔI) of the carbocyanine probe diSC$_3$-(5) and the magnitude of the imposed K^+ diffusion potential in both mollicutes. ΔI proved linearly related to $\Delta\Psi$ between -95 and -7 mV in *A. laidlawii* and -123 and -21 mV in *S. melliferum*, which allowed a fairly good estimation of membrane potential variations induced in these bacteria by peptide treatment.

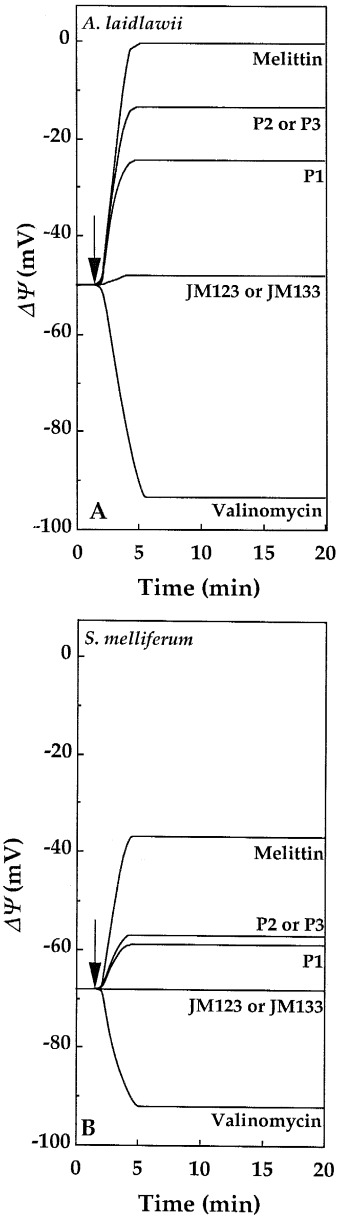

Fig. 5. Effect of peptides on membrane electrical potential ($\Delta\Psi$) in *A. laidlawii* A-PG8(A) and *S. melliferum* BC3 (B). The arrows indicate the time at which the peptides were added to the cell suspensions. Concentrations used: 1 μM for valinomycin and 0.1 μM for the other peptides. Each curve is the average of at least three independent measurements (SD ≤ ±8.5%).

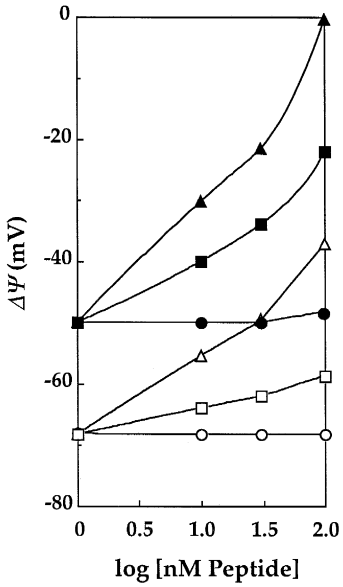

Fig. 6. Effect of peptide concentration on the alteration of membrane potential in *A. laidlawii* A-PG8 (A) and *S. melliferum* BC3 (B). Each point is the average of at least three distinct measurements (SD ≤ ±8.5%). Symbols: melittin (△ and ▲), P1 (□ and ■), JM133 (○ and ●), *A. laidlawii* (▲, ■, and ●), and *S. melliferum* (△, □, and ○).

The fluorescence signal observed after the addition of the probe to cell suspensions reached a constant level after about 1 min. In the absence of peptide, a steady fluorescence signal was recorded over at least 20 min, indicating that both *A. laidlawii* and *S. melliferum* were capable of maintaining a constant membrane potential in buffer containing 50 mM glucose (Fig. 5). This membrane potential was of -50 mV in *A. laidlawii* (Fig. 5A) and -68 mV in *S. melliferum* (Fig. 5B). Treatment of the cells with 0.1 μM melittin induced a depolarization of the plasma membrane in both *A. laidlawii* ($\Delta\Psi$ dropped from -50 to 0 mV, i.e., $\Delta[\Delta\Psi] = 50$ mV) and *S. melliferum* ($\Delta[\Delta\Psi] = 31$ mV). The peptides P1, P2, and P3 (0.1 μM) also depolarised the membranes of *A.*

laidlawii ($\Delta[\Delta\Psi] = 25$ mV for P1 and 36 mV for P2 and P3) and *S. melliferum* ($\Delta[\Delta\Psi] = 9$ mV for P1 and 11 mV for P2 and P3), but to a lesser extent than melittin. JM123 and JM133 were devoid of significant activity when used at the same concentration than melittin or P-series peptides since they induced a drop of $\Delta\Psi$ of only 2 mV in *A. laidlawii* whereas no effect could be measured in *S. melliferum*. Fig. 6 further shows the dose-dependence of peptide-induced membrane depolarisation in *A. laidlawii* and *S. melliferum*.

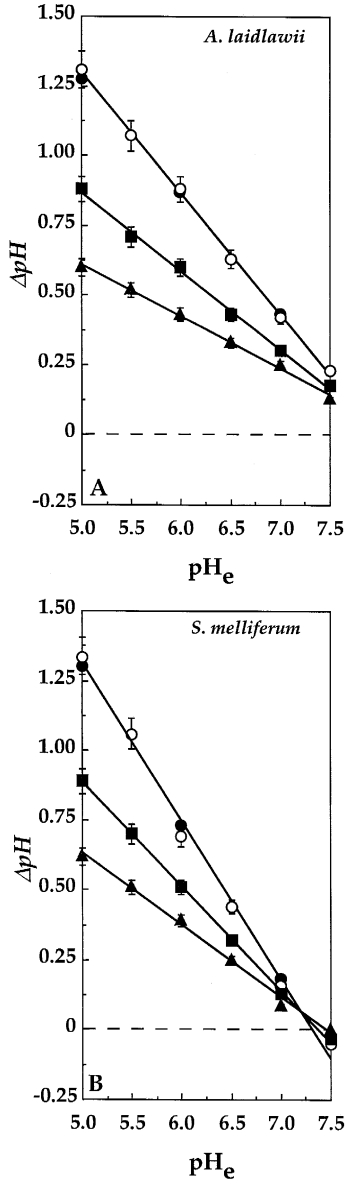

Fig. 7. Effect of peptide-treatment on the transmembrane pH gradient. The intracellular pH (pH_{in}) of cells energised with 50 mM glucose was determined as described in Section 2. $\Delta pH = pH_{in} - pH_{out}$, with each point being the average of at least three independent measurements (SD $\leq \pm 3\%$). Each peptide was used at a concentration of 0.1 μM. Symbols: untreated cells (○) and cells treated with melittin (▲), P1 (■), or JM133 (●).

3.5. Effect of the peptides on transmembrane ΔpH

The effect on the transmembrane pH gradient ($\Delta pH = pH_{in} - pH_{out}$) was thoroughly analysed for melittin, P1, and JM133 (Fig. 7). *A. laidlawii* and *S. melliferum* energised with 50 mM glucose were capable of maintaining a ΔpH ($pH_{in} - pH_{out} > 0$) which proved to be stable for at least 20 min. This transmembrane gradient increased linearly from 0.23 to 1.31 in *A. laidlawii* (Fig. 7A) and from 0 to 1.34 in *S. melliferum* (Fig. 7B) as the external pH was diminished from 7.5 to 5.0. Immediately after the addition of peptide (0.1 μM melittin or P1), the ΔpH increased transiently for about 2 min and then dropped within 2 min to reach a steady value, always lower than that observed in the absence of peptide. As expected from $\Delta\Psi$ measurements (see above), P1 diminished the ΔpH in both mollicutes, but less efficiently than melittin, whilst no effect could be detected with JM133.

4. Discussion

The antibiotic activity of the synthetic peptides was assessed by growth inhibition tests using six species of mollicutes: *A. laidlawii* which is frequently found as a contaminant in animal tissue cell cultures [33], *M. gallisepticum* which is pathogenic for poultry [34], *M. genitalium* which might be associated with non-gonococcal urethritis in humans [35], *M. mycoides* ssp. *mycoides* SC which is responsible for contagious pleuropneumonia in cattle [36], *S. citri*, the agent of 'stubborn' disease of citrus [37], and the honeybee pathogen *S. melliferum*. A comparison of the MICs determined for the different peptides (Table 2) shows that among the molecules used in this work, P-series peptides were thoroughly more active than JM-series peptides. It is noteworthy that in the case of *A. laidlawii*, P2 and P3 were more

potent than P1, and JM133 more potent than JM123. A comparison of the sequences of these peptides (Fig. 1) suggests that shortening the linker between the hydrophobic *N*-terminal sequence and the polycationic *C*-terminal stretch KKKRK was responsible for a two-fold increase of the antibiotic activities. However, the activities of the synthetic peptides were much lower than those of melittin. In particular, none of the six mollicutes was capable of resisting the effect of the bee-venom peptide whereas *M. mycoides* ssp. *mycoides*s SC was resistant to all of the synthetic peptides at concentrations up to 100 μM. The higher resistance of *M. mycoides* ssp. *mycoides* SC to the synthetic peptides and melittin, and to other natural peptides [19] might well be due to the presence of a capsule of galactan on the surface of this mollicute [38]. Indeed, this capsule appears as a major difference between the surfaces of *M. mycoides* ssp. *mycoides* SC and the other species used in this study. Conversely, the presence of large amounts of spiralin on the cell surface of spiroplasmas [39–42] does not seem to protect these mollicutes against membrane-seeking peptides. However, to clearly assess the protective functions of the capsule and of spiralin, comparisons with galactan-defective mutants of *M. mycoides* ssp. *mycoides* SC and spiralin-defective mutants of spiroplasmas need to be performed.

Spiroplasma cell motility and helicity being very sensitive to membrane-seeking peptides [19], we have used *S. melliferum* BC3 to further investigate the antibacterial activities of the peptides. P1 and JM133 were both capable of deforming *S. melliferum* cells but were again much less potent than melittin. The deforming power of the peptides actually paralleled their growth inhibition activities. The analysis of the effects on the membrane electrical potential ($\Delta\Psi$) and the transmembrane pH gradient (ΔpH) of *A. laidlawii* and *S. melliferum* revealed that P-series peptides were capable of decreasing $\Delta\Psi$ (i.e., making the membrane potential less negative) and ΔpH, but less efficiently than melittin, whereas no effect could be recorded with JM-series peptides (Figs. 5–7). These data suggest that both types of peptides are membranotoxic but only the former have a significant ionophoric activity in mollicutes. They also suggest that the MICs determined by the growth inhibition test in liquid medium probably underestimate the antibiotic activity of peptides since much lower concentrations were needed to deform spiroplasma cells or to de-energise the plasma membrane. This might be due to the fact that MICs were determined in culture media whilst cell deformation experiments and measurements of $\Delta\Psi$ and ΔpH were performed in cells dispersed in buffer. Since culture media for mollicutes are complex and usually contain animal serum, lipoproteins thus supplied to the media may compete with membranes as targets for the peptides.

Two main mechanisms have been proposed so far to explain the lytic activity of melittin (for reviews see [12,43]): (i) The α-helical peptides bind parallel to the membrane surface and lysis occurs upon the subsequent formation of transmembrane bundles of helices delineating hydrophillic pores (‘barrel stave’ model) and (ii) the adsorbed peptides stay oriented parallel to the surface of the membrane and destabilise this one by burying the helix hydrophobic face into the lipid bilayer (‘wedge’ model). Both mechanisms induce ion leakage and subsequent membrane lysis. In addition, it is known that at high enough peptide/lipid ratios and under appropriate conditions, melittin disrupts membranes into small discs surrounded by a peptide shell, according to a detergent-like effect [10]. In fact, melittin can probably adopt these different states when interacting with membranes and several factors including notably the lipid/mellitin ratio will favour one of these topologies [11].

It was beyond the scope of the present work to elucidate the mechanism of peptide/membrane interaction in mollicutes. Nevertheless, some clues were provided by the different studies. CD spectroscopy data (Fig. 2A–B, and Table 1) indicate that P-series peptides adopted a mainly β-sheet conformation in the presence of liposomes whereas in the same conditions, turns appeared to be the major conformation in JM-series peptides. If we assume that the conformations of the peptides in biomembranes are similar to those observed in liposomes, one may infer that the mechanisms responsible for the toxicity of P-series and JM-series peptides are different from those described for melittin (see above) since, in the same conditions, mellitin is essentially α-helical (reviewed in [11]). This interpretation is consistent with the fact that *A. laidlawii* membrane thickness had no influ-

ence on the antibiotic activity of the synthetic peptides whilst that of mellitin was inversely related to membrane thickness (Table 3). However, it should be noted that even if the activity of melittin depended on the average thickness of the bilayer, it was still very high (MIC = 3.12 μM) on cells exhibiting the thickest membrane hydrophobic core (i.e., 28 Å). This is consistent with the observation that melittin interacts with lipids of different acyl chain lengths provided that the interaction is initiated in the lipid fluid phase [44], which is the case of mollicutes observed at their optimal growth temperature.

Furthermore, P-series and JM-series were responsible for spiroplasma cell agglutination, a phenomenon which was not observed with melittin. The agglutination of the cells by P1 and JM133 suggests that at least a fraction of these peptides interacted with the plasma membrane in such a way that the polycationic *C*-terminus was exposed on the surface of the cells, allowing thus the formation of intercellular ionic bridges. As expected, this phenomenon was strongly enhanced by increasing the cell/peptide ratio.

In conclusion, this study shows that the bactericidal activities of melittin and of the synthetic peptides analysed here were directly related to their ability in abolishing the transmembrane electrochemical potential. It remains however to elucidate the molecular mechanism responsible for the alteration of membrane permeability. This question will be addressed using NMR spectroscopy for structural investigations and planar lipid bilayers to analyse membrane permeabilisation. Furthermore, we consider the possibility of improving the antibacterial activity of the synthetic peptides by derivatisating their *C*-terminal cysteamide function.

Acknowledgements

This work was supported by the Langlois Foundation, the 'Groupement de Recherches Peptides et Protéines Amphipathiques' (GDR 1153, CNRS), and the 'Ministère de l'Education Nationale, de l'Enseignement Supérieur et de la Recherche' (ACC 'Physico-Chimie des Membranes Biologiques'). LC was supported by the ANRS. We are grateful to Dr. Åke Wieslander for helpful suggestions and for the gift of *A. laidlawii* A-EF22 cells adapted to grow in media with different fatty acid compositions. We thank the members of the GDR No. 1153 for many stimulating discussions and Marie-Madeleine Guéguen for skilful technical assistance.

References

[1] W.F. Broekaert, F.R.G. Terras, B.P.A. Cammue, R.W. Osborn, Plant Physiol. 108 (1995) 1353–1358.
[2] W.L. Duax, J.F. Griffin, D.A. Langs, G.D. Smith, P. Grochulski, V. Pletnev, V. Ivanov, Biopolymers 40 (1996) 141–155.
[3] J.A. Hoffmann, C. Hétru, Immunol. Today 13 (1992) 411–415.
[4] B.L. Kagan, T. Ganz, R.I. Lehrer, Toxicology 87 (1994) 131–149.
[5] R. Maget-Dana, F. Peypoux, Toxicology 87 (1994) 151–174.
[6] W.L. Maloy, U.P. Kari, Biopolymers 37 (1995) 105–122.
[7] P. Nicolas, A. Mor, Annu. Rev. Microbiol. 49 (1995) 277–304.
[8] A.G. Rao, Mol. Plant-Microbe Interaction 8 (1995) 6–13.
[9] H. Kleinkauf, H. Von Döhren, Eur. J. Biochem. 236 (1996) 335–351.
[10] J. Dufourcq, J.-F. Faucon, G. Fourche, J.-L. Dasseux, M. Le Maire, T. Gulik-Krzywicki, Biochim. Biophys. Acta 859 (1986) 33–48.
[11] I. Cornut, E. Thiaudière, J. Dufourcq, In: R.M. Epand (Ed.), The Amphipathic Helix, CRC Press, Boca Raton, 1993, pp. 173–219.
[12] I. Cornut, K. Büttner, J.-L. Dasseux, J. Dufourcq, FEBS Lett. 349 (1994) 29–33.
[13] D. Kalderon, W.D. Richardson, A.F. Markham, A.E. Smith, Nature 311 (1984) 33–38.
[14] C. Dingwall, R.A. Laskey, Tr. Biochem. Sci. 16 (1991) 478–481.
[15] J. Maniloff, In: J. Maniloff, R.N. McElhaney, L.R. Finch, J.B. Baseman (Eds.), Mycoplasmas: Molecular Biology and Pathogenesis, ASM Press, Washington, DC, 1992, pp. 549–559.
[16] S. Razin, FEMS Microbiol. Lett. 100 (1992) 423–432.
[17] S. Razin, In: J. Maniloff, R.N. McElhaney, L.R. Finch, J.B. Baseman (Eds.), Mycoplasmas: Molecular Biology and Pathogenesis, ASM Press, Washington, DC, 1992, pp. 3–22.
[18] L. Béven, M. Le Hénaff, C. Fontenelle, H. Wróblewski, Curr. Microbiol. 33 (1996) 317–322.
[19] L. Béven, H. Wróblewski, Res. Microbiol. 148 (1997) 163–175.
[20] V.E. Habermann, J. Jentsch, Hoppe–Seyler's Z. Physiol. Chem. 348 (1967) 37–50.
[21] J. Méry, J. Brugidou, J. Derancourt, Pept. Res. 5 (1992) 233–240.
[22] J. Méry, C. Granier, M. Juin, J. Brugidou, Int. J. Pept. Protein Res. 42 (1993) 44–52.

[23] P. Vidal, L. Chaloin, J. Méry, N. Lautredou, R. Bennes, F. Heitz, J. Pept. Sci. 2 (1996) 125–133.
[24] R.L. Thurmond, A.R. Niemi, G. Lindblom, Å. Wieslander, L. Rilfors, Biochemistry 33 (1994) 13178–13188.
[25] U. Schummer, H.-G. Schiefer, In: S. Razin, J.G. Tully, Molecular and Diagnostic Procedures in Mycoplasmology, Academic Press, New York, 1995, pp. 251–263.
[26] A.S. Waggoner, Annu. Rev. Biophys. Bioeng. 8 (1979) 47–68.
[27] L. Letellier, E. Shechter, Eur. J. Biochem. 102 (1979) 441–447.
[28] J.B. Stock, B. Rauch, S. Roseman, J. Biol. Chem. 252 (1977) 7850–7851.
[29] P. Breeuweur, J.-L. Drocourt, F.M. Rombouts, T. Abee, Appl. Environ. Microbiol. 62 (1996) 178–183.
[30] O.H. Lowry, N.J. Rosebrough, A.L. Farr, R.J. Randall, J. Biol. Chem. 193 (1951) 265–275.
[31] M.A.K. Markwell, S.M. Hass, L.L. Bieder, N.E. Tolbert, Anal. Biochem. 87 (1978) 206–210.
[32] W.R. Gallaher, Cell 50 (1987) 327–328.
[33] G.J. McGarrity, H. Kotani, G.H. Butler, In: J. Maniloff, R.N. McElhaney, L.R. Finch, J.B. Baseman (Eds.), Mycoplasmas: Molecular Biology and Pathogenesis ASM Press, Washington, D.C., 1992, pp. 445–454.
[34] T.B. Clark, R.F. Whitcomb, J.G. Tully, C. Mouchès, C. Saillard, J.M. Bové, H. Wróblewski, P. Carle, D.L. Rose, R.B. Henegar, D.L. Williamson, Int. J. Syst. Bacteriol. 35 (1985) 296–308.
[35] J.G. Tully, D. Taylor-Robinson, D.L. Rose, R.M. Cole, J.M. Bové, Int. J. Syst. Bacteriol. 33 (1983) 387–396.
[36] A. Provost, P. Perreau, A. Bréard, C. Le Goff, J.L. Martel, G.S. Cottew, Rev. Sci. Tech. Off. Int. Epiz. 6 (1987) 625–679.
[37] P. Saglio, M. L'hospital, D. Laflèche, G. Dupont, J.M. Bové, J.G. Tully, E.A. Freundt, Int. J. Syst. Bacteriol. 23 (1973) 191–204.
[38] P. Plackett, S.H. Buttery, Biochem. J. 9 (1964) 201–205.
[39] Å. Wieslander, M.J. Boyer, H. Wróblewski, In: J. Maniloff, R.N. McElhaney, L.R. Finch, J.B. Baseman (Eds.), Mycoplasmas: molecular biology and pathogenesis, ASM Press, Washington, DC, 1992, pp. 93–112,
[40] H. Wróblewski, K.-E. Johansson, S. Hjertén, Biochim. Biophys. Acta 465 (1977) 275–289.
[41] H. Wróblewski, S. Nyström, A. Blanchard, Å. Wieslander, J. Bacteriol. 171 (1989) 5039–5047.
[42] C. Brenner, H. Duclohier, V. Krchnák, H. Wróblewski, Biochim. Biophys. Acta 1235 (1995) 161–168.
[43] C.E. Dempsey, Biochim. Biophys. Acta 1031 (1996) 143–161.
[44] J.-F. Faucon, J.-M. Bonmatin, J. Dufourcq, E.J. Dufourc, Biochim. Biophys. Acta 1234 (1995) 235–243.